Electronic Supplementary Material (ESI) for Nanoscale.

Supplementary information

1. Composition of the nanoparticles

SI Table 1. Detailed composition of the synthetic batches for the preparation of the NPs.

NP batch	Template	Monomers***			Cross-linker****
		MAA	Aam	TBAm	BIS
MIP-CC9ox	CC9 ox*	49 µL	41 µL	37 µL	875 µL
MIP-CC9alk	CC9 alk**	49 µL	41 µL	37 µL	875 µL
NIPs	-	49 µL	41 µL	37 µL	875 µL

* peptide CC9ox had sequence CGGGHRSKC, structured in a cycle upon the formation of the cystine bond between the two terminal cysteines.
** CC9alk was CC9 alkylated to block the cysteine from reacting; alkylating agent for the two cysteines was iodoacetamide (alkylation mechanism reported below).
*** Monomer stock solutions were 2% (w/v)
**** BIS stock solution was 2% (w/v)

MAA, methacrylic acid; Aam, Acrylamide; TBAm, Ter-butyl-acrylamide; BIS, N, N'-methylenebisacrylamide

Iodoacetamide alkylation mechanism.

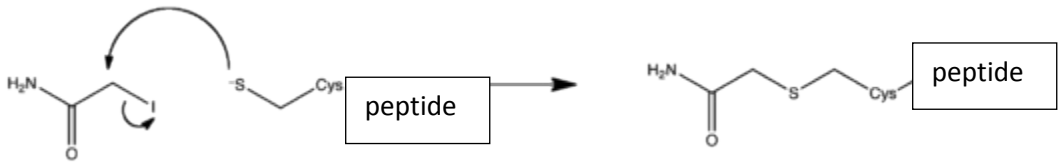

Smythe C.V. J. Biol. Chem. 1936, 114 (3): 601–12.

2. Dynamic Light Scattering

SI Table 2. DLS measurements of the NPs.

Nanoparticle	Z-average (nm)	PDI
MIP-CC9ox	34 ± 1	0.2
MIP-CC9alk	27 ± 1	0.2
NIP	36 ± 1	0.2

3. Scanning Electron Microscopy of the nanoparticles

SI Table 3. Exemplificative statistical analysis of the SEM image of MIP-CC9ox NPs.

	N total	Mean	Minimum	Median	Maximum
Major	203	48 ± 19	17	46	103
Minor	203	42 ± 17	11	40	96

4. XPS analysis

XPS analyses were performed on a Kratos AXIS Supra (XPS) surface analysis instrument UltraDLD (Shimadzu, Japan). The analysis conditions were: Primary beam X-ray mono Al K; Primary beam energy 1486.6 eV; Take off angle 0°; Energy resolution 0.4 eV; Neutralizer on.
Initially each sample was surveyed in the binding energy interval -2, 1300 eV. Afterwards the core levels C 1s of O 1s, N 1s and Si 2p were collected at higher energy resolution. A neutralizer was used to compensate the sample charges. The binding energies were referenced to C-C/C-H bond at 285.0 eV.

SI Table 4. Elemental composition of the NPs synthesized.

Sample	O (%)	N (%)	C (%)
MIP-CC9ox	17.3	16.1	66.7
MIP-CCalk	16.4	16.0	67.6
NIP	16.3	16.0	67.7

5. Isothermal Titration Calorimetry data

SI Figure 1: A, B: thermogram and molar heats obtained by the titration of CC9ox 17 µM with MIP-CC9ox NPs.

A B

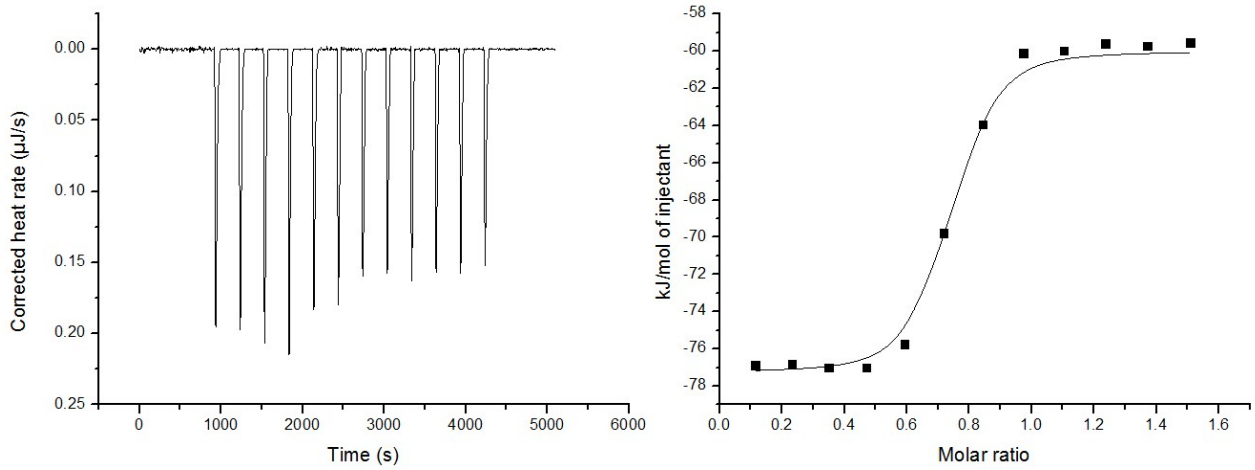

SI Figure 2: A, B: thermogram and molar heats obtained by the titration of CC9ox 17 µM with MIP-CC9alk NPs.

A

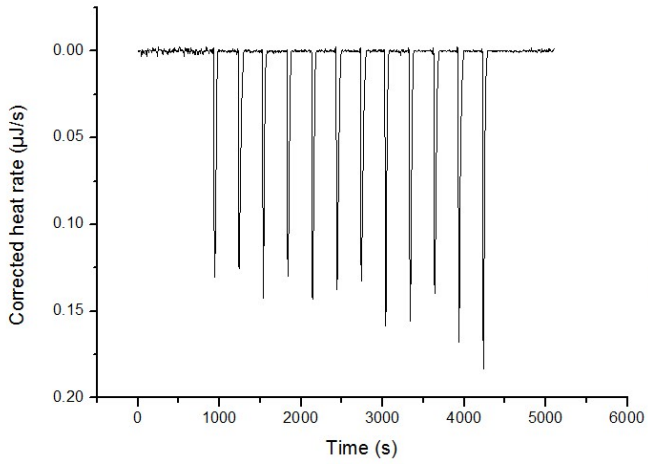

B

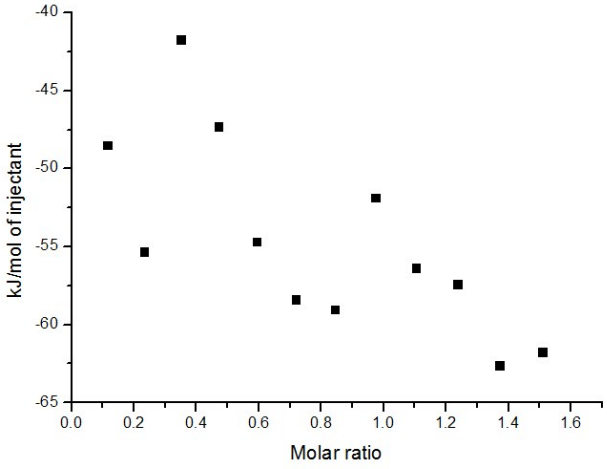

SI Figure 3: A, B: thermogram and molar heats obtained by the titration of CC9ox 17 μM with NIP-NPs.

A

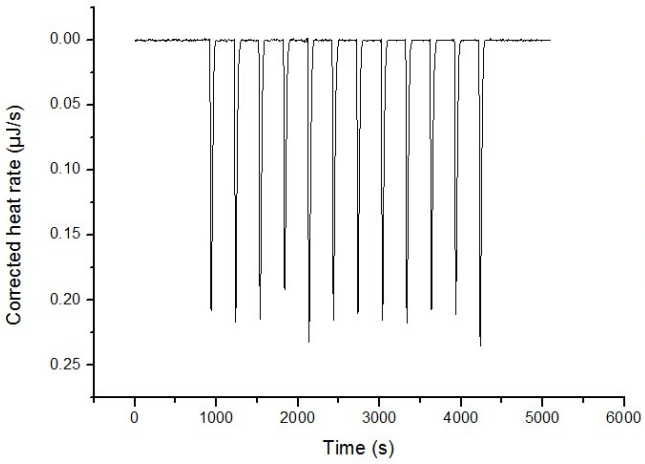

B

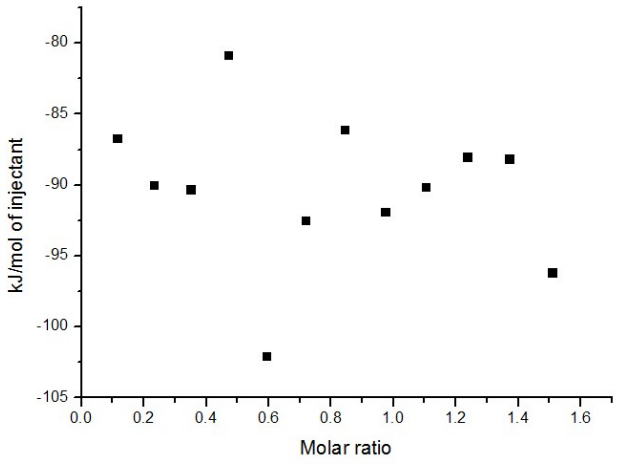

SI Figure 4: A, B: thermogram and molar heats obtained by the titration of Hepcidin-25 17 µM with MIP-CC9ox NPs.

A B

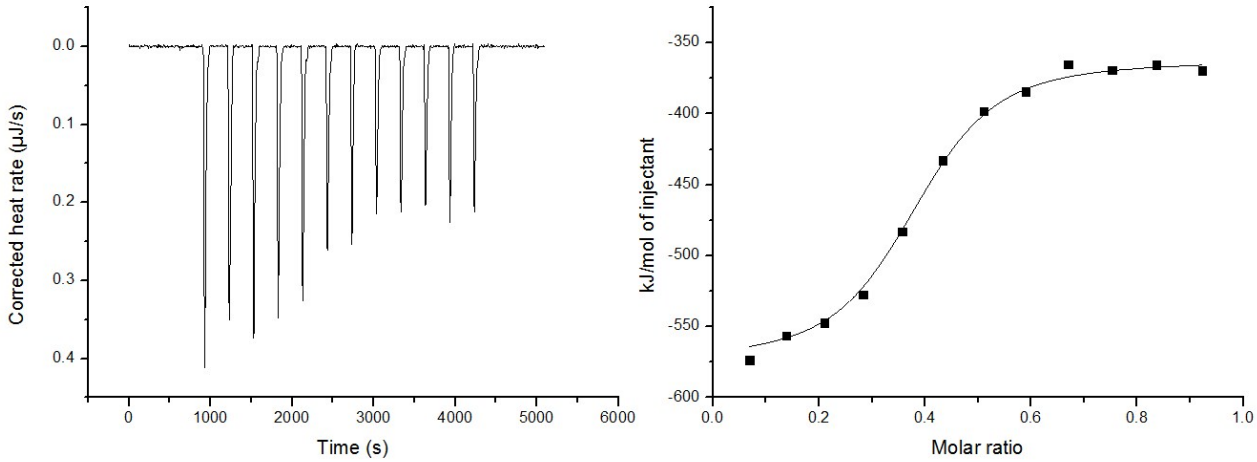

SI Figure 5: A, B: thermogram and molar heats obtained by the titration of Hepcidin-20 17 µM with MIP-CC9ox NPs.

A B

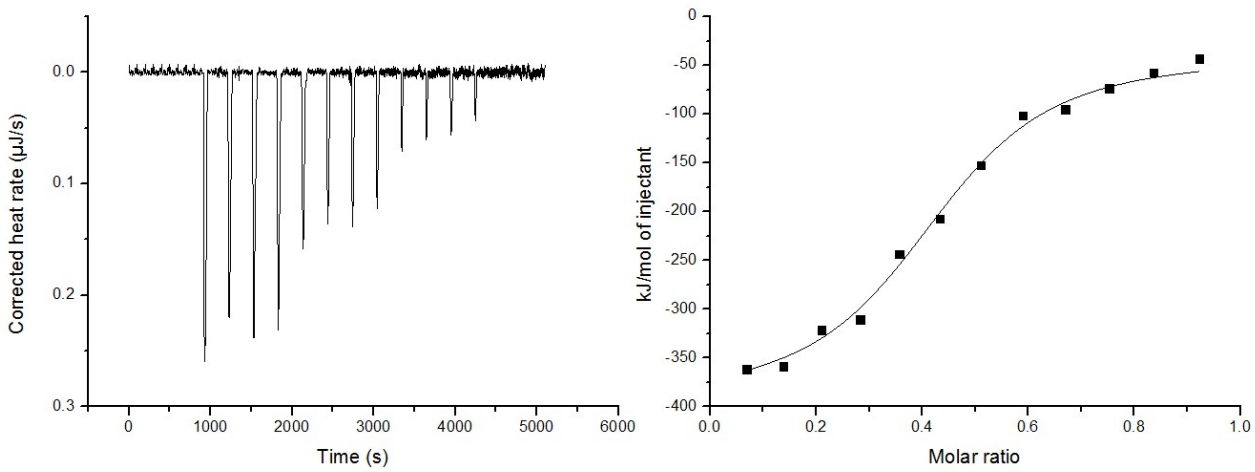

SI Figure 6: A, B: thermogram and molar heats obtained by the titration of peptide NR10 (sequence: NIDALGMEGR, 1162.28 g/mol, pI 4.37) 17 μM with MIP-CC9ox NPs.

A B

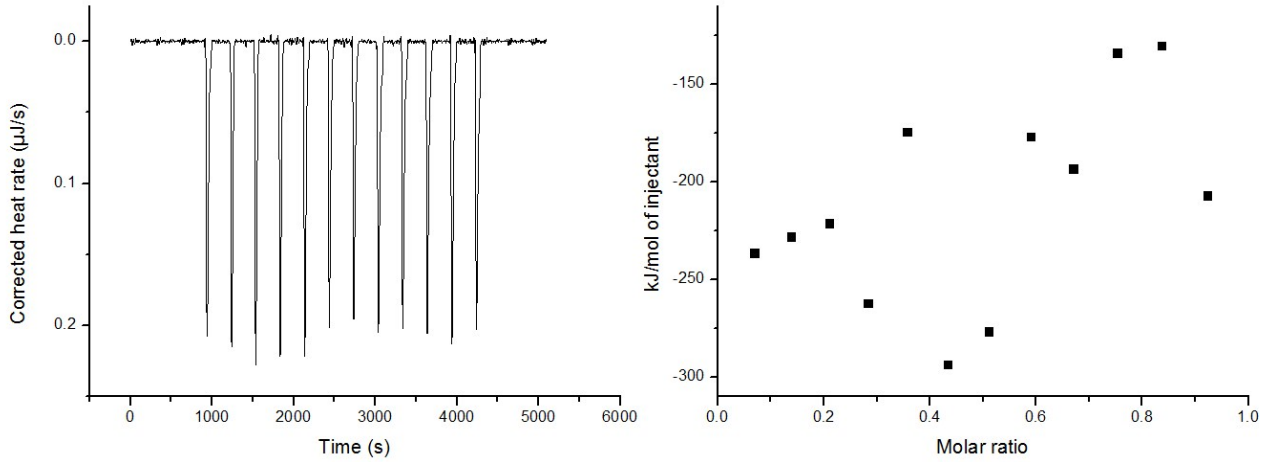

6. MALDI-TOF MS of CC9red and CC9ox

For peptide analysis 2,5 dihydroxybenzoic acid (DHB) (Sigma Aldrich, Milan, Italy) organic matrix was used 20 mg/mL in acetonitrile:water 30:70 v/v, 0.1% TFA. Equal volumes (0.5 µL) of matrix and sample were mixed, deposited onto a ground steel target and let to air-dry. Peptide MALDI-TOF-MS measurements were conducted on an Ultraflex II instrument (BrukerDaltonik GmbH, Leipzig, Germany) operating under FlexControl 3.0 software. Spectra were acquired in the positive ion-mode (detection by reflectron) at a laser frequency of 20 Hz and within a mass range from 100 to 4000 Dalton; matrix suppression by deflection was set at 100 Da. The laser wavelength was 337 nm. Ion source 1 (IS1) voltage was set at 25 kV, IS2 at 21.5 kV, lens at 9.30 kV, reflectron at 26.30 kV, reflectron 2 at 13.80 kV and detector gain was 6.8 x. Pulsed ion extraction was 50 ns. For each sample spot, one sum spectrum was accumulated from 500 measurements on different spot locations. Samples were prepared at least in triplicate.

SI Figure 7: MALDI spectrum of CC9ox (red line) and CC9red (black line) peptides.

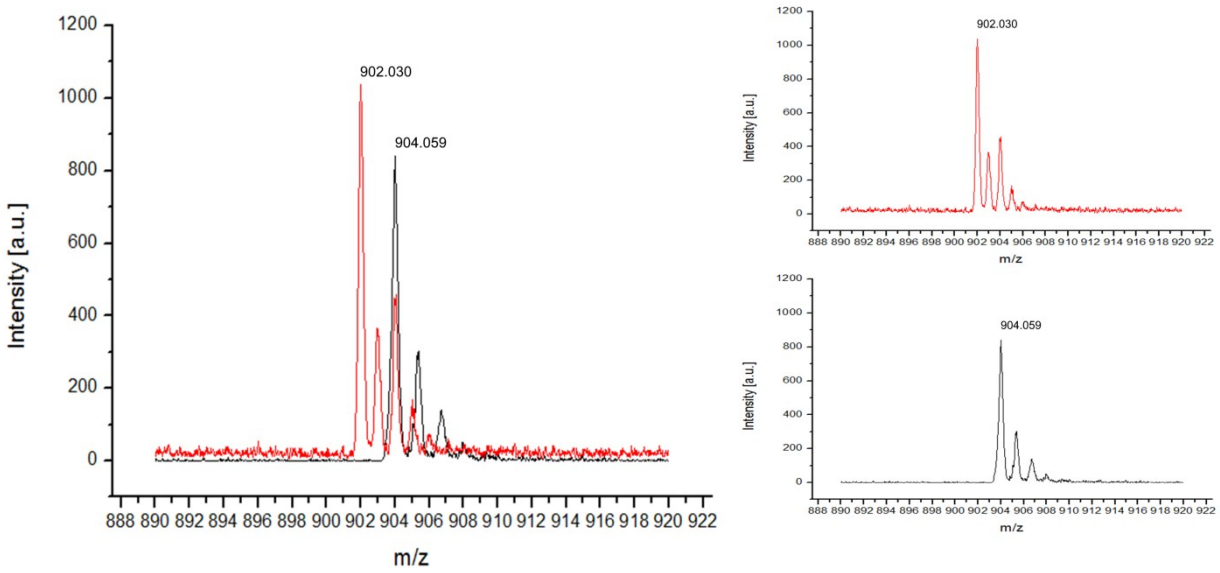

7. NMR of the CC9red and CC9ox forms

SI Figure 8: ^{1}H-NMR spectra taken at time = 0 and time = 3h showing the conversion of CC9red (cysteine signals at δ_H 2.84) into CC9ox peptide (cystine signals at δ_H 3.24)

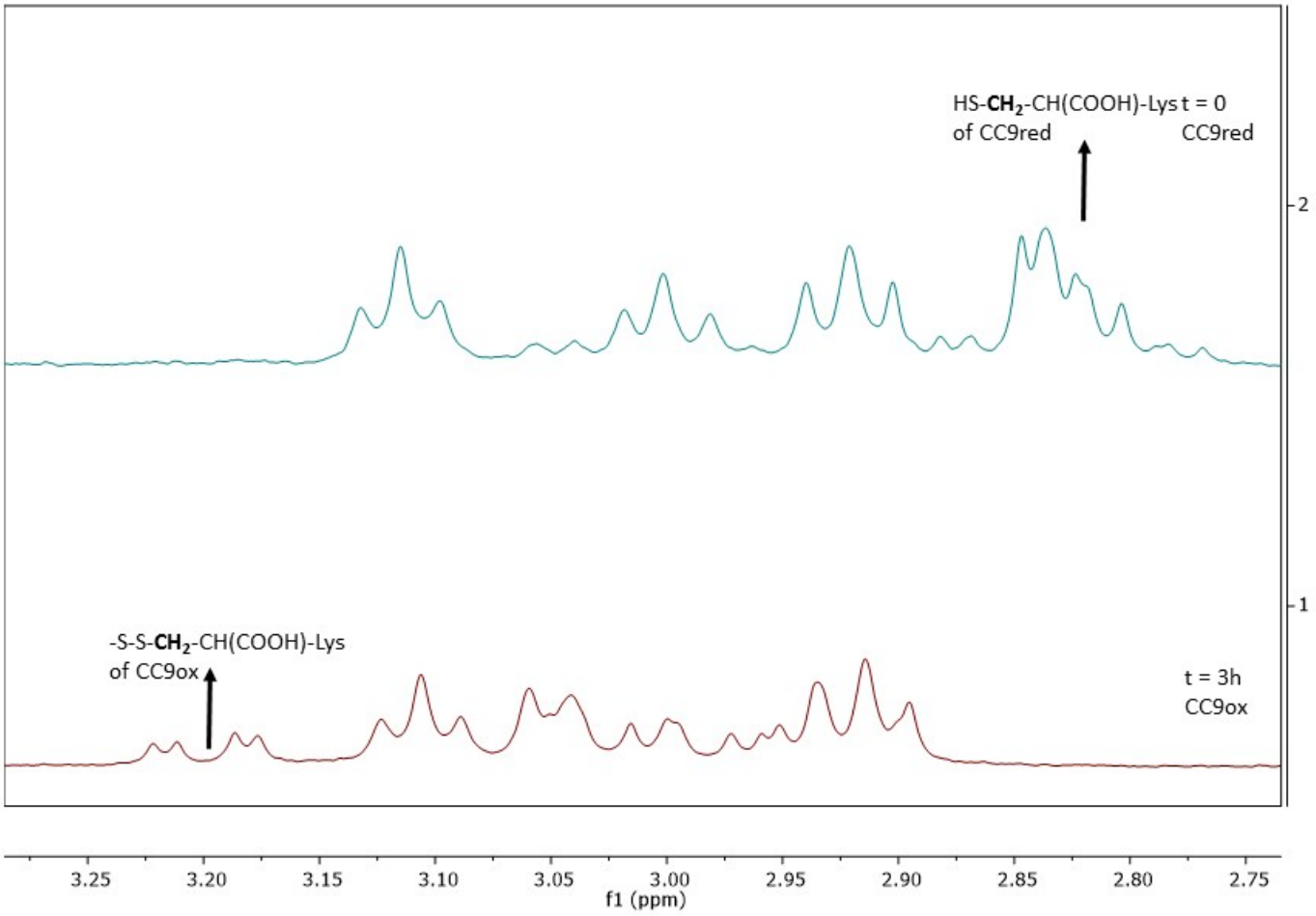

8. HPLC for the CC9 oxidation kinetic

SI Figure 9: HPLC profiles of the process of CC9 oxidation. CCred elutes at RT = 8.1 min; CC9ox elute at RT = 6.2 min.

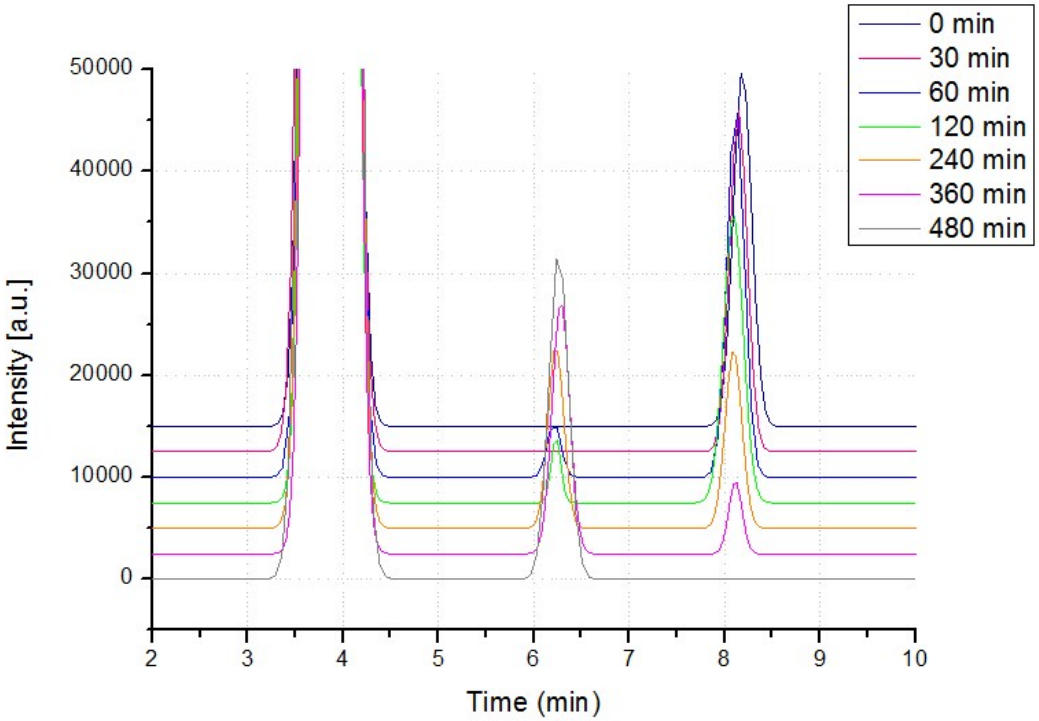

SI Table 5: CC9red oxidation

% CC9red				
Time (min)	**No NPs**	**MIP-CC9ox**	**MIP-CC9alk**	**NIP**
0	100	100	100	100
1	100	67 ± 5	73 ± 1	78 ± 5
3	100	44 ± 7	54 ± 5	56 ± 2
5	100	28 ± 5	33 ± 8	36 ± 4
6	100	16 ± 1	-	36 ± 5
8	100	0	-	24 ± 4
10	100	0	20 ± 2	17 ± 5
12	100	0	-	6 ± 3
13	100	0	4 ± 3	4 ± 2
15	100	0	0	0
30	99 ± 1	0	0	0
60	98 ± 2	0	0	0
120	80 ± 2	0	0	0
180	67 ± 3	0	0	0
240	54 ± 4	0	0	0
300	41 ± 3	0	0	0
360	27 ± 4	0	0	0
420	16 ± 7	0	0	0
480	5 ± 5	0	0	0
540	0	0	0	0

SI Figure 10: Time course of the oxidation of CC9red (100 µM) in the presence of 1 µM MIP-CC9ox NPs (grey ☒) or 1 µM NIP NPs (patterned ⭘). The slopes of the curves were: -0.0662 for NIP NPs ($R^2 = 0.9920$) and -0.1165 for MIP-CC9ox NPs ($R^2 = 0.9927$).

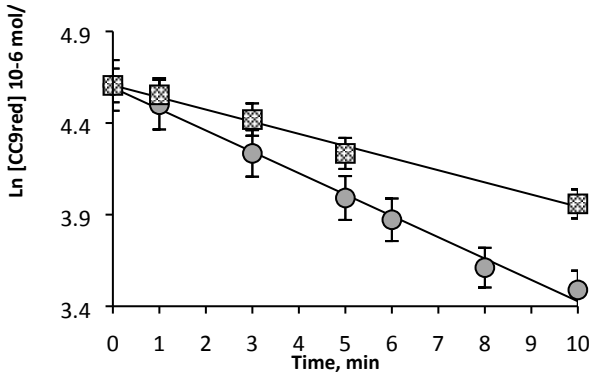

SI Figure 11: Time course of the oxidation of CC9red (100 µM) in the presence of 1 µM MIP-CC9ox NPs (grey ☒) or 1 µM NIP NPs (patterned ⭘).

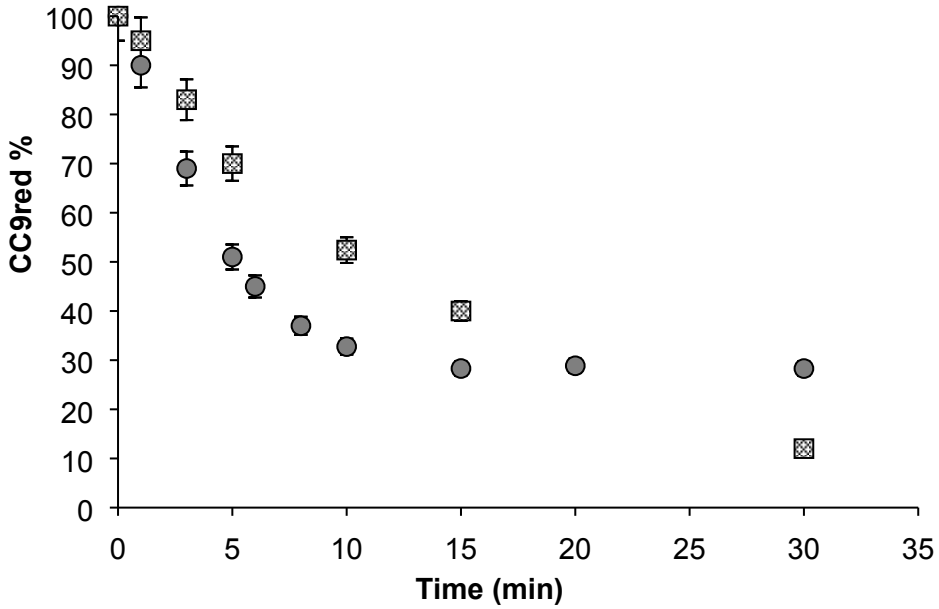

9. LC-MS of the CC9red and CC9ox

SI Figure 12: Top : LC-UV (λ=204 nm) of the CC9red oxidation (after 30 min) showing both CC9red and CC9ox forms. Bottom: ESI positive ion-mode MS spectra of CC9ox (t_R = 3.7 min) and CC9red (t_R = 4.9 min) showing the corresponding protonated ions (and ion-adducts) at the m/z values 902.5 (CC9ox) and 904.5 Da (CC9red) as expected from their corresponding molecular formula.